

1 Pervasive occurrence of microplastics in Hudson-Raritan estuary zooplankton

2

3 Authors and affiliations:

4

5 Karli Sipps^a, Georgia Arbuckle-Keil^a, Robert Chant^b, Nicole Fahrenfeld^c, Lori Garzio^b, Kasey
6 Walsh^b, Grace Saba^{b,*}

7

8 ^a Department of Chemistry, Rutgers, The State University of New Jersey, Camden, NJ, 08102,
9 USA

10 ^b Department of Marine and Coastal Sciences, Rutgers, The State University of New Jersey, New
11 Brunswick, NJ, 08901, USA G. Saba: saba@marine.rutgers.edu, * Corresponding author

12 ^c Department of Civil & Environmental Engineering, Rutgers, The State University of New
13 Jersey, Piscataway, NJ, 08854, USA

14

15

* Corresponding author: Department of Marine and Coastal Sciences, Rutgers, The State University of New Jersey, New Brunswick, NJ, 08901, USA. *Email address:* saba@marine.rutgers.edu (G. Saba)

16 ABSTRACT

17

18 Microplastics (MP) are considered emerging contaminants in the water environment, and there is
19 an interest in understanding their entry into the food web. As a growing body of literature
20 demonstrates the ingestion of MP by zooplankton in controlled laboratory studies, few data are
21 available demonstrating *in situ* observations of MP in zooplankton. A field survey was
22 performed to collect zooplankton in the highly urbanized Hudson-Raritan estuary. Following
23 washing, sorting by species, and enumeration, three dominant species of copepods (*Acartia*
24 *tonsa*, *Paracalanus crassirostris* and *Centropages typicus*) were digested. MP were filter
25 concentrated and characterized by size, morphology, and color via microscopy and polymer type
26 by micro-FTIR imaging and/or Raman spectroscopy. MP were observed in all extracts
27 performed on the three copepod species with averages ranging from 0.30 to 0.82 MP individual⁻¹.
28 Polyethylene and polypropylene were the dominant polymer types observed and fragments and
29 beads the most commonly observed morphologies for MP. These data were used to estimate the
30 flux of MP through zooplankton based on gut turnover times, which we compare to estimates of
31 MP entering this environment through the local waterways. The estimated fluxes were
32 sufficiently large, indicating that ingestion by zooplankton is a major sink of MP in the size
33 range subject to zooplankton feeding in surface estuarine waters.

34

35 Keywords: plastics, copepods, polymer, Raman micro-spectroscopy

36

37 **1. Introduction**

38
39 Plastic pollution in aquatic environments is an increasingly important concern. The human
40 population produces an average of about 1.5 megatons of plastic waste every year (Boucher and
41 Friot, 2017). Plastic waste not recycled, combusted for energy recovery, or properly landfilled
42 (representing an estimated 8.7%, 15.8%, and 75.6% of US plastics generated in 2018,
43 respectively) can enter the land and water environment where most of this plastic will not break
44 down completely (United States Environmental Protection Agency, 2021), but rather will be
45 subject to mechanical or photo oxidative degradation processes that will lead to the
46 fragmentation of the macroscopic plastics into microscopic plastic particles (Andrady, 2011).
47 These particles, categorized as microplastics (hereafter, MP), are defined as plastic fragments
48 that are 5 mm or less in diameter. The tendency for discarded plastic products to ultimately end
49 up in waterways is primarily responsible for the ubiquity of MP in lakes (Dusaucy et al., 2021;
50 Iannilli et al., 2020; Pastorino et al., 2021), rivers (Nel et al., 2018; Ravit et al., 2017), estuaries
51 and coasts (Bailey et al., 2021; Frias et al. 2014; Rodrigues et al., 2019; Zhao et al. 2014), the
52 open ocean (Cózar et al. 2014; Moore et al. 2001), and deep-sea sediments (Kanhai et al. 2019;
53 Woodall et al. 2014) from tropical to polar ecosystems (Alfaro-Núñez et al., 2021; Burns and
54 Boxall, 2018; Waller et al. 2017). Regions identified as most at risk from MP pollution, estuaries
55 and the coastal ocean, are those exposed a high number of MP sources (Cole et al., 2011). MP
56 concentrations up to 2.75 microplastic/m³ for 500-2000µm and 4.71 microplastic/m³ for 250-
57 500µm were recently reported from the mouth of the Raritan River out to the coastal ocean
58 (Bailey et al., 2021). Generally, concentrations of macro and microplastics in lakes, rivers, and
59 oceans have been reported between 10⁻³-10³ microplastic/m³ (Alimi et al., 2018), the variation

60 being a function not only of study location but also methods, with higher concentrations
61 observed when smaller particles and more morphologies were included in analyses.

62
63 MP that pollute the aquatic environment may enter the food chain through consumption by
64 organisms that inhabit terrestrial, water column (pelagic), and benthic environments such as
65 semiterrestrial amphipods, zooplankton, fish, crabs, and shellfish (Farrell and Nelson, 2013;
66 Iannilli et al., 2020; Savoca et al., 2021; Setälä et al., 2014; Van Colen et al., 2020). Zooplankton
67 are particularly susceptible to MP ingestion due to similarity in size and density (i.e., buoyancy)
68 of their natural prey sources (Costa et al., 2020; Rodrigues et al., 2021; Zheng et al., 2020), and
69 the presence of MP has been detected in 28 taxonomic orders encompassing nearly 40 species,
70 including several different copepods (Zheng et al., 2020). Furthermore, biofilm formation on the
71 surface of aged MP has been reported to increase the attractiveness of particles as food for
72 zooplankton (Vroom et al., 2017), but can also serve to change the buoyancy of MP particles and
73 therefore impact their fate in aquatic environments.

74
75 MP can pose many threats to marine organisms (Avio et al., 2016; Botterell et al., 2019; Derraik,
76 2002; Foley et al., 2018; Wright et al., 2013). In zooplankton, MP ingestion has been associated
77 with decreases in survival (Lee et al., 2013; Svetlichny et al., 2021; Yu et al., 2020; Zhang et al.,
78 2019), development and growth (Cole et al., 2019; Jeong et al., 2017), fecundity (Jeong et al.,
79 2017; Zhang et al., 2019), and egg hatching success (Cole et al., 2015). Furthermore, plastic
80 additives or monomers can be hazardous, impact mobility, development, and reproduction of
81 zooplankton (Botterell et al., 2019; Cole et al., 2011; Lee et al., 2013).

82

83 Although an increasing number of studies have focused on the relationship between MP and
84 zooplankton, most published results are from laboratory settings rather than field collection
85 involving the digestion of whole zooplankton to quantify all MP ingested (Rodrigues et al.,
86 2021). Of those field studies, research in the open ocean predominates and thus is not
87 representative of MP-zooplankton relationships in highly populated, biologically productive
88 coastal systems. The discrepancy between the number of laboratory versus field studies is likely
89 a result of the methodological challenges of extracting and analyzing environmental MP from
90 environmental organisms. Laboratory studies typically use colored or fluorescent MP beads or
91 fragments that can be visually inspected in organism guts or stomachs once ingested. Visual
92 identification of these colored or fluorescently labeled plastics is possible. However, the
93 detection and analysis of small MP ingested by zooplankton in natural systems. requires
94 chemical digestions of collected organisms, ideally optimized to reduce non-target debris from
95 the organism without altering the polymers targeted. A second challenge is analysis of the
96 extracted particles, which even with optimized protocols still contain non-anthropogenic debris,
97 and for the size range relevant to ingestion by zooplankton, use analytical techniques that are
98 more challenging than for large particles. Chemical analysis of MP can be performed by FTIR
99 and Raman spectroscopy, techniques that are non-destructive and require minimal sample
100 preparation after particles have been extracted from the environmental matrix. For particles
101 smaller than 500 μm , a microscope is commonly coupled to the spectrometer. Raman
102 spectroscopy has a lower diffraction limit; hence, smaller particles ($< 15 \mu\text{m}$) can be accurately
103 identified.

104

105 Interactions between MP and marine organisms is facilitated in coastal waters because of
106 enhanced MP pollution and high organism abundance (Clark et al., 2016; Sun et al., 2018a). The
107 few studies that have examined MP ingested by zooplankton in natural seawater highlighted the
108 ubiquity of occurrence, but also demonstrated high variability in ingestion incidence and MP
109 characteristics in terms of size, morphology, and polymer type (Desforges et al., 2015; Kosore et
110 al., 2018; Sun et al., 2018a, b; Taha et al., 2021; Zheng et al., 2020). Additionally, there have
111 been no published studies reporting *in situ* ingestion of MP by zooplankton in the Hudson-
112 Raritan estuary (Fig. 1), the location of interest in the present study. We note that in addition to
113 being highly urbanized, this system is of historical significance because General Bakelite, the
114 first company in the world to produce synthetic plastic opened up at the mouth of the Raritan in
115 Perth Amboy in 1909 (Crespy et al., 2008). Finally, ingestion of MP by zooplankton may
116 represent a major sink of MP in the marine environment (Kvale et al., 2020), but to our
117 knowledge there are no system-scale estimates of the fraction of MP discharged into an estuary
118 or coastal system that are ingested by zooplankton.

119
120 Here we present the first comprehensive characterization of MP ingested by planktonic copepods
121 in the highly urbanized Hudson-Raritan Estuary (Fig. 1) using micro-FTIR imaging and/or
122 Raman spectroscopy. We predicted that the MP ingestion incidence by zooplankton would be
123 high. Therefore, the objective of this study was to determine MP ingestion incidence and
124 characterize MP ingested by multiple species of zooplankton by size, morphology, color and
125 polymer type. The field campaign included a single day field effort in July 2018 to test and
126 develop protocols followed by a two-day effort in April of 2019. Sampling was performed along
127 a salinity gradient on these three dates that also exhibited different flow conditions. This strategy

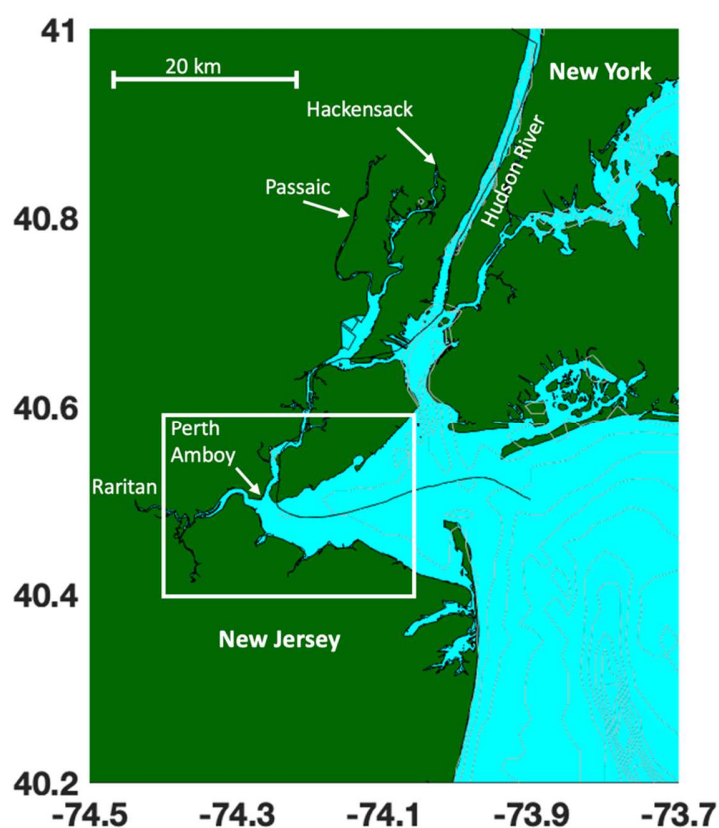
128 allowed us to test the potential effects of these parameters on MP ingestion. Comparisons were
129 also made to water column MP concentration and polymer profile observations previously
130 reported (Bailey et al., 2020). These data were used to estimate the flux of MP through
131 zooplankton based on gut turnover times, which we compared to estimates of MP entering this
132 environment through the local waterways.

133

134 2. Materials and methods

135

136 2.1. Sampling area



137

138 **Fig 1.** Map of the Hudson-Raritan Estuary. Latitude in decimal degrees North, Longitude in
139 degrees West. White box represents sampling area depicted in Figure 2. Solid black line
140 designates state boundary between New Jersey and New York.

141
142 The present study was performed in a highly urbanized estuary where MP pollution may be
143 significant due to the proximity to high-population areas. The Hudson-Raritan watershed is home
144 to nearly five million people and hundreds of various aquatic species, making the environmental
145 impact of MP of particular importance (New York State Office of the Attorney General, 2015).

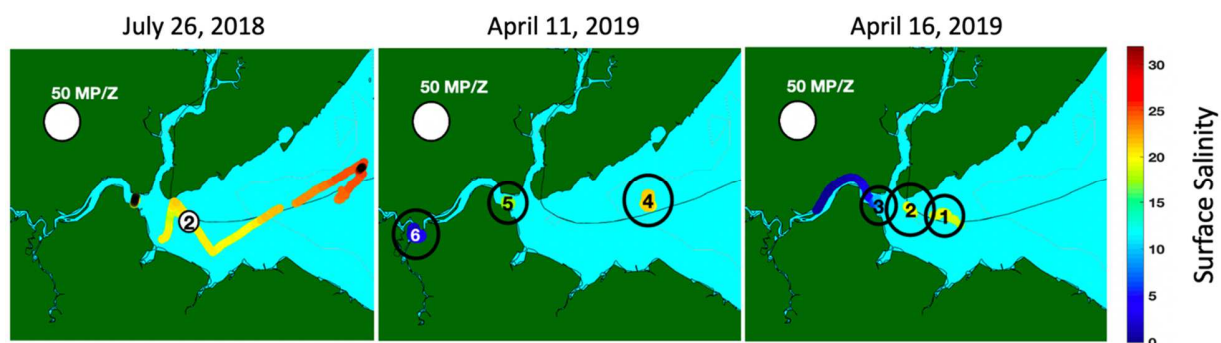
146

147 *2.2. Sample collection*

148

149 Paired samples to determine and characterized MP in water and in zooplankton were collected
150 aboard the R/V Rutgers on one date in July 2018 and two sampling dates in April 2019 (Fig.
151 2). Sampling dates were selected to capture different flow conditions: low flow (July 2018),
152 moderate flow (April 11, 2019), and high flow (April 16, 2019) (Bailey et al. 2021). Sampling
153 was performed along the salinity gradient, based on real time salinity data from a flow through
154 CTD aboard the ship, at sites in Raritan River (4/11/19 Site 6), at the river mouth (4/11/19 Site 5;
155 4/16/19 Site 3), and at frontal locations within the estuary (7/26/18 Site 2; 4/11/19 Site 4; 4/16/19
156 Sites 1 and 2). The characterization of MP in surface water, from samples collected using nets,
157 for these locations has been previously reported (Bailey et al., 2021). Briefly, duplicate 20.3 cm
158 diameter ring nets (mesh size 80 or 150 μm , Science First, Yulee, FL) were used to collect
159 buoyant particles at the water surface at each sampling site. Collected samples were wet sieved,
160 and particles were subjected to wet peroxide oxidation followed by density separation with
161 sodium chloride (NaCl; Masura et al., 2015), buoyant particles were filtered on to 63 μm
162 stainless steel wire mesh (TWP, Berkeley, CA) and analyzed via FTIR and/or Raman
163 spectroscopy.

164



165

166 **Fig. 2.** Bubble plots displaying the average number of MP extracted per 100 zooplankton (MP/Z)
 167 across the sampling sites. The number inside of each bubble indicates the sampling site number,
 168 and the color corresponds to surface salinity at each site. Average MP values were calculated
 169 based on two replicates from 4/16 Site 2 and three replicates of all other samples. Solid black
 170 line designates state boundary between New Jersey and New York.

171

172 Duplicate surface tows for zooplankton were conducted at each site using 0.5 m ring net with
 173 200 μm mesh and fitted with flowmeters (General Oceanics, Model 2030R) at the net openings
 174 and filtering cod-ends. Nets were towed for approximately 5 minutes at a speed of 1-2 knots. The
 175 contents of the cod-ends were then rinsed with filtered seawater from the cod-ends into glass
 176 collection jars and preserved in a 10% buffered formalin solution until analysis.

177

178 2.3. Extraction of MP from zooplankton

179

180 Subsets of zooplankton were removed from preserved sample jars and concentrated on a 200 μm
 181 sieve while rinsing with 0.2 μm MilliQ water (MilliporeSigma). Processing small sample
 182 aliquots at a time, zooplankton were then rinsed into glass petri dishes and examined under a

183 dissecting microscope. Copepods were sorted and morphologically identified by species. The
184 dominant species observed in each sample, determined via microscopic analysis using the
185 preserved sample from the duplicate tow (see Section 3.1), were targeted for MP digestion and
186 analysis. These included *Acartia tonsa*, *Centropages typicus*, and *Paracalanus crassirostris*.
187 Individual copepods were rinsed copiously with 0.2 µm filtered MilliQ water and inspected
188 microscopically for any MP attached to their appendages or exoskeleton. If detected, external
189 particles were removed using steel forceps. After cleaning and inspection, copepods were placed
190 in 7 ml glass scintillation vials with PTFE-lined caps in sets of 100 individuals of the same
191 species per vial, or sample. Triplicate samples (each with 100 copepods) for each sampling date
192 and study site, with the exception of duplicate samples for April 16 Site 2, were prepared. Each
193 sample was digested in 3 mL of concentrated (70%) nitric acid at 80° C for two hours (Desforges
194 et al., 2015). Samples were then diluted with 0.2 µm MilliQ water in a 1:1 ratio and filtered onto
195 0.2 µm pore size 25 mm Anodisc membranes (Whatman) under low vacuum. Filters were rinsed
196 with additional MilliQ water and then placed into glass petri dishes with glass lids. Procedural
197 blanks (7 mL vials filled only with 3 mL of the nitric acid digesting agent) and a matrix blank
198 spiked with 15 µm polystyrene beads were performed alongside each digestion. The matrix blank
199 was prepared by diluting a white coloured polystyrene microbead stock solution (Sigma #74964)
200 with 0.2 µm MilliQ water such that the final concentration of beads in each matrix blank sample
201 (N=2) was calculated to be approximately 50 beads. These microbeads were selected because
202 they were available in a comparable size to the environmental particles we expected to be
203 extracted from the copepods and are easily quantifiable.

204

205 Due to the high particle counts, random subsampling (25% - 90% of total filter area analyzed) of
206 each filter was performed. Particles were observed to be uniformly distributed across the filters,
207 and MP totals were determined by scaling up the numbers of MP detected in each subsection to
208 represent 100% of the filters. Subsampled MP were enumerated, measured for size, and
209 characterized for color, morphology, and composition (polymer type) through visual (described
210 in section 2.4) and chemical (described in section 2.5) analyses. MP ingestion incidence,
211 reported here as MP individual⁻¹, was calculated by dividing MP counts on each filter by 100
212 individuals. Average and standard deviation (SD) of ingestion incidence were calculated from
213 the replicate samples processed from each sampling date and study site.

214

215 *2.4. Visual analysis*

216

217 Visual characteristics, such as color and morphology, as well as the size of each particle were
218 documented prior to spectral acquisition. Particle morphologies were classified as either beads,
219 fragments, or films. The few fibers observed were omitted from this study due to the possibility
220 of aerial contamination (Wesch et al., 2017; Woodall et al., 2015). The size of each particle was
221 measured on the Raman microscope using the distance and profile measurement tool in Horiba's
222 LabSpec software (Version 6.5). All sizes were reported as the length of the longest axis of the
223 particle.

224

225 *2.5. Chemical analysis & spectral interpretation*

226

227 Recalcitrant particles remaining following the digestion were analyzed for MP content using
228 micro-FTIR imaging and/or Raman microscopy. An effort was made to collect both IR and
229 Raman spectra for all samples. However, IR was not successful on all MP and therefore some
230 samples were limited to the collection of Raman spectra only.

231
232 Each sample was analyzed directly on the Anodisc membrane, an appropriate substrate for both
233 spectroscopic techniques that were utilized. Micro-FTIR imaging was performed using a Bruker
234 Hyperion 3000 FTIR microscope (Bruker Optics, Billerica, MA) equipped with a 64x64 element
235 focal plane array (FPA) detector and a 15x IR microscope objective. All spectra were collected
236 in transmission mode in the wavenumber region of 4000 - 1250 cm^{-1} due to absorbance features
237 from the filters below 1250 cm^{-1} that would interfere with sample spectra. Open air was used as a
238 background, and all spectra were acquired with 32 background scans and 32 sample scans at a
239 spectral resolution of 8 cm^{-1} . False-color images were then generated by integration of the 3000 -
240 2800 cm^{-1} (aliphatic C-H stretching) spectral region in order to identify probable organic
241 particles. Positions of these particles relative to the center of the filter were noted, and
242 subsequent Raman spectroscopic analysis was performed to confirm potential MP.

243
244 Raman analysis was conducted using a Horiba XploRA PLUS confocal Raman microscope
245 equipped with 532, 638, and 785 nm excitation wavelengths and 10x [numerical aperture (N.A.)
246 = 0.25], 50x LWD (N.A. = 0.50) and 100x (N.A. = 0.90) microscope objectives. Measurement
247 parameters were adjusted for each sample to optimize the signal-to-noise ratio and maximize the
248 quality of the spectra. Raman spectra were evaluated through a combination of manual
249 interpretation (Socrates, 2004) and spectral searching programs OpenSpecy (Cowger et al., 2021)

250 and BioRad KnowItAll (Academic Edition). When an exact determination of polymer type could
251 not be made, MP were classified broadly (e.g., polyester or epoxy resin) according to the
252 functional groups and linkages present in the sample.

253

254 *2.6. Data analysis*

255

256 Statistical analysis was performed using R (www.rproject.org). ANOVA was used to compare
257 the total MP per copepod as a function of sampling date and species with a post-hoc Tukey test.
258 A Shapiro test was used to confirm the normality of MP counts per copepod. The distributions of
259 polymer types found in surface seawater and in copepods were square root transformed, a Bray-
260 Curtis dissimilarity matrix was calculated, and results are presented via non-metric
261 multidimensional scaling (nDMS). ANOSIM was performed to test for differences in the
262 polymer profiles using a nested approach for matrix (surface seawater vs. in copepod) and
263 sampling date. ANOSIM was also performed to compare the MP particle size profiles observed
264 in the copepod samples between site and date. Spearman rank correlations were tested between
265 MP abundance per 100 copepods and MP concentrations previously reported in the water
266 column in the 250-500 μm and 500-2000 μm size range.

267

268 To quantify the fraction of MP entering the Hudson-Raritan system that are ingested by
269 zooplankton, we estimated the volume of MP discharged into the system based on prior studies
270 and the flux of MP through the zooplankton community. To estimate the flux of MP into the
271 system, we used data from Meijer et al. (2021) who estimated the mean USA loadings of MP to
272 the ocean to be 7.4 Tons of MP million people⁻¹ and scaled that to the population in the Hudson-

273 Raritan watershed. To estimate flux of MP through zooplankton, we first estimated the mean
 274 volume of plastics per zooplankton, V_p , as

$$275 \quad V_p = \frac{\alpha \sum_{i=1}^n N_i L_i^3}{N_z} \quad (1)$$

276 where α is a shape factor, defined as the ratio of the longest dimension of MP to the shortest
 277 dimension, and is taken from the literature (Cózar et al., 2014), N_i is the number of plastics
 278 reported in each of $n=5$ size classes, L_i is the size class, and $N_z=2000$ is the total number of
 279 zooplankton sampled. For L_i , we chose the mid-point for $i=2$ to 4 (i.e., 17.5 μm , 37.5 μm , and
 280 75 μm) and the minimum (i.e., 10 μm) and maximum (i.e., 100 μm) for $i=1$ and 5, respectively.
 281 The flux of MP through zooplankton is the ratio of our estimate of V_p to gut retention time, and
 282 this is discussed in more detail in the results and discussion.

283

284 **3. Results**

285

286 *3.1. Zooplankton abundance and community composition*

287

288 A total of 28 zooplankton taxa were identified in net tows conducted in the Hudson-Raritan
 289 study location. Total zooplankton present in the study location ranged from 58-5771 individuals
 290 m^{-3} , and were highly variable between sampling date and site (Table 1). Copepods comprised 70-
 291 98% (mean \pm SD = 89 \pm 10%) of the total zooplankton present in the collected samples in the
 292 study area. These abundance values are within range of those reported in the study location
 293 previously (Jeffries, 1964; Rothenberger et al., 2014; Stepien et al., 1981). Although the highest
 294 abundance of copepods occurred at the highest measured salinity, there was no significant linear
 295 correlation between salinity and abundance ($p = 0.28$). Among copepods, two species/genera

296 were present in all samples processed (*Acartia tonsa* and *Paracalanus* spp.), and *Centropages*
 297 *typicus* was present in all but two samples. When present, these three species/genera were
 298 typically the most abundant. A few exceptions occurred. For instance, *Eurytemora* spp. were
 299 most abundant at one sampling date and site (4/16/2019 Site 4); however, they were only present
 300 in three of the processed samples. Within genus *Paracalanus*, dominance fluctuated between *P.*
 301 *crassirostris* and *P. parvus*; however, we selected only *P. crassirostris* for the MP analysis for
 302 consistency as this was the species that dominated in the samples that were processed first. *A.*
 303 *tonsa*, *C. typicus*, and *P. crassirostris* were therefore the three copepod species targeted for MP
 304 analyses in the present study.

305

306 **Table 1.** Abundance of zooplankton, and specifically copepods, in the Hudson-Raritan study
 307 location. Abundance of total copepods includes the younger copepodite life stages. The
 308 abundance of select copepods includes only the three copepod species that were persistent and
 309 typically the dominant adult stages in the processed tow samples and therefore used in the MP
 310 analyses (*Acartia tonsa*, *Centropages typicus*, and *Paracalanus crassirostris*).

311

Sampling Date and Site	Total Zooplankton (individuals m ⁻³)	Total Copepods (individuals m ⁻³)	Select Copepods (individuals m ⁻³)
7/26/2018 Site 2	58	41	32
4/11/2019 Site 4	95	86	57
Site 5	426	416	288
Site 6	1462	1386	885
4/16/2019 Site 1	5771	5305	3381
Site 2	503	485	335
Site 3	1308	1089	100

312

313 3.2. Total MP content in copepods

314

315 Three species of copepods (*A. tonsa*, *P. crassirostris* and *C. typicus*) were targeted, and MP were
 316 detected in all 20 samples analyzed (Table 2 and Fig. 3; Each ‘sample’ represents 100
 317 individuals). Average ingestion incidence (MP individual⁻¹) in the study area ranged from 0.30-
 318 0.82 (Table 2). No significant differences were observed in total MP extracted from the copepods
 319 between species (ANOVA, all $p > 0.35$, Table 2) or between the two April sampling dates ($p =$
 320 0.65), but total MP extracted from copepods was significantly lower in the July 2018 samples
 321 compared to samples from the two April 2019 dates (ANOVA, both $p < 0.009$). Furthermore, no
 322 significant correlation between site-specific copepod abundance and ingestion incidence was
 323 observed, suggesting that the amount of MP found within zooplankton was not dependent upon
 324 zooplankton abundance.

325
 326 **Table 2.** MP ingestion incidence of target copepod species in the Hudson-Raritan study location.
 327 Dominant zooplankton species were targeted for MP analysis at each study site (*Acartia tonsa*,
 328 *Centropages typicus*, and *Paracalanus crassirostris*). Ingestion Incidence (MP individual⁻¹) was
 329 calculated from number of MP per 100 copepods and reported here as an average \pm standard
 330 deviation (SD) at each study site. Averages and SDs were calculated based on two replicates
 331 from 4/16 Site 2 and three replicates of all other samples.

332

Sampling Date and Site	Zooplankton Species	Ingestion Incidence (MP individual ⁻¹) Average \pm SD
7/26/2018 Site 2	<i>A. tonsa</i>	0.30 \pm 0.07
4/11/2019 Site 4	<i>A. tonsa</i>	0.73 \pm 0.09
Site 5	<i>P. crassirostris</i>	0.60 \pm 0.08
Site 6	<i>P. crassirostris</i>	0.74 \pm 0.14
4/16/2019 Site 1	<i>A. tonsa</i>	0.69 \pm 0.13
Site 2	<i>C. typicus</i>	0.82 \pm 0.48
Site 3	<i>A. tonsa</i>	0.51 \pm 0.14

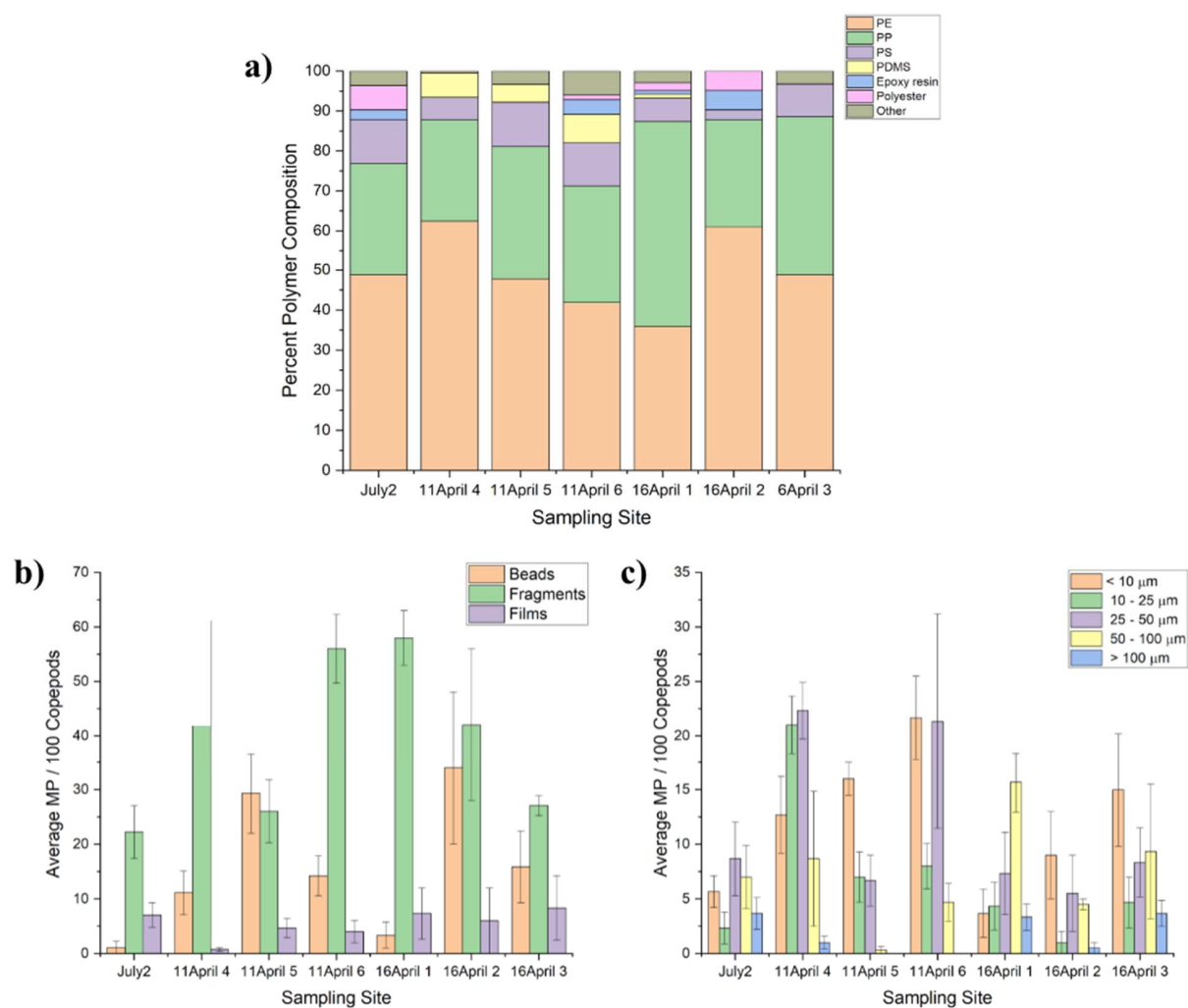
333

334 *3.3. MP characterization and size-structure in copepods*

335

336 Polyethylene and polypropylene were the most commonly observed polymer types across all
337 copepod samples, followed by polystyrene. Polyesters, such as polyethylene terephthalate (PET),
338 as well as polydimethylsiloxane (PDMS) rubber and other polymers, including epoxy resins and
339 vinyl copolymers were also observed (Fig. 3). No differences in polymer profiles were observed
340 between the sampling sites or dates (ANOSIM, all $p \geq 0.10$) with replicates clustering with
341 51.7% (Site 2, July 26 and April 16) to 80.1% (Site 6, April 11) similarity.

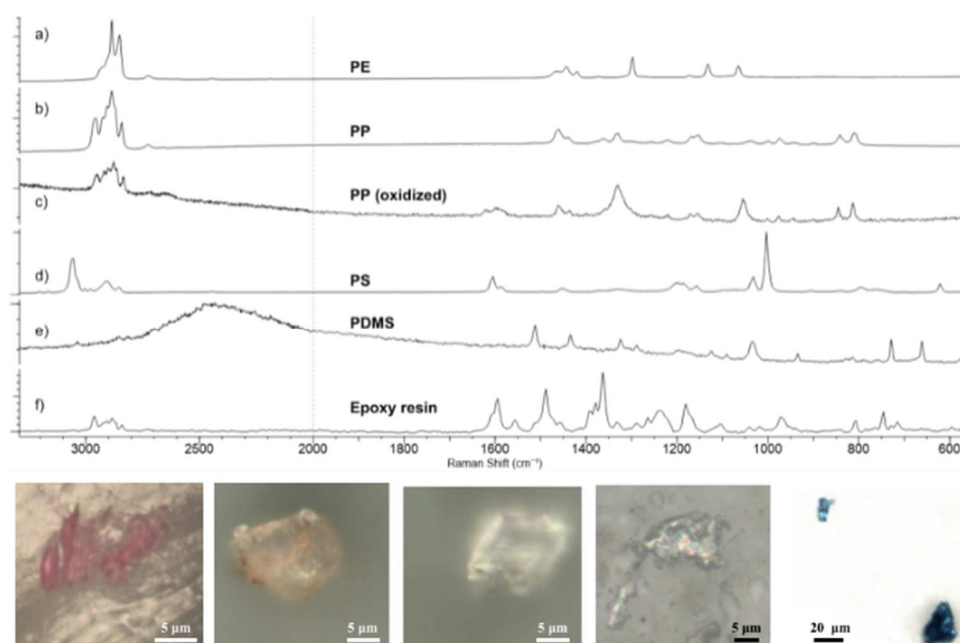
342



343
 344 **Fig 3.** Characterization and size of MP found in copepods collected from the Hudson-Raritan
 345 study site. (a) Percentage of polymer types in the total MP, (b) average MP per 100 copepods by
 346 morphology, and (c) average MP per 100 copepods for different size classes extracted from
 347 copepods collected from each sampling site. Sampling site names are listed by Day Month Site.
 348 Average values are reported for N=2-3 replicates per site.

349
 350 Raman spectra of common polymers, such as polyethylene (Fig. 4a) and polystyrene (Fig. 4d),
 351 could typically be evaluated on sight. The Raman spectra of most polypropylene MP indicated
 352 extensive polymer oxidation (Fig. 4c), as evidenced by the introduction of bands at

353 approximately 1300 cm^{-1} and $1050 - 1000\text{ cm}^{-1}$, which can be correlated with oxygen-containing
354 functional groups. PDMS MP (Fig. 4e) were identified by key bands at 1440 cm^{-1} (CH_3
355 deformation), 1050 cm^{-1} (Si-O-Si symmetric stretch), 810 cm^{-1} (Si-C stretch) and 575 cm^{-1} (Si-O-
356 Si asymmetric stretch). Similarly, epoxy resins (Fig. 4f) were identified by key bands at 1500
357 cm^{-1} (CH_2 deformation), 1250 cm^{-1} (epoxide C-O stretch), 810 cm^{-1} (ring vibration) and 750 cm^{-1}
358 (ring vibration). Pigmented polyethylene and polypropylene MP were observed in a variety of
359 colors, including red (Fig. 4), green, blue, purple and orange. All epoxy resin particles were blue
360 (Fig. 4). Overall, colorless or gray/brown MP were most abundant ($> 75\%$ of all MP observed).
361 Six out of seven procedural blanks were confirmed to be free of MP, with the exception of fibers
362 greater than $400\text{ }\mu\text{m}$ in size. Two $15\text{ }\mu\text{m}$ polystyrene beads were found on one of the blanks.
363 Accordingly, $15\text{ }\mu\text{m}$ polystyrene beads found on any subsequent samples were omitted from
364 average MP counts. A recovery of 54% was reported for the matrix spike.
365



366

367 **Fig. 4.** Representative Raman spectra and images of MP observed in Hudson-Raritan estuary
368 copepods. Top: Representative Raman spectra of (a) polyethylene, (b) polypropylene, (c)
369 oxidized polypropylene, (d) polystyrene, (e) polydimethylsiloxane and (f) epoxy resin MP.
370 Bottom: Example MP images, from left to right, are polyethylene, polypropylene, polystyrene,
371 polydimethylsiloxane, and epoxy resin (both blue particles). All images were captured using a
372 100x microscope objective.

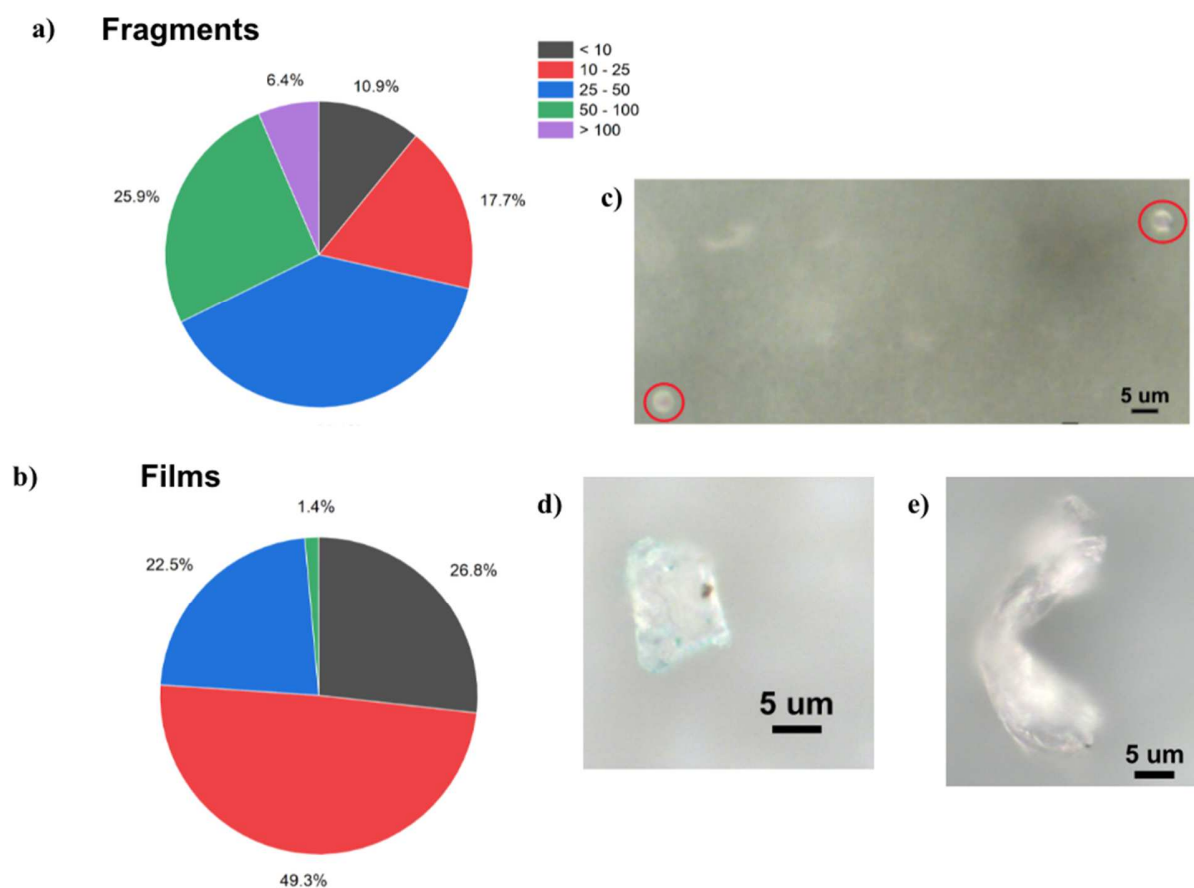
373

374 Fragments were the most commonly observed morphology found in the digested copepod
375 samples in all but one site (Fig. 3b) (4/11/2019 Site 5). Beads were the dominant morphology
376 found in copepods collected from the mouth of the Raritan River on 4/11/2019 (Site 5) and were
377 also found in relatively high amounts in copepods collected near this location on 4/16/2019
378 (Sites 2 and 3). It is noteworthy that, although fibers were intentionally excluded from MP
379 analysis, no fibers within the expected size range of particles ingested by the copepods analyzed
380 were observed.

381

382 All beads were measured to be 5 μm in diameter and spectroscopically determined to be
383 polyethylene. Films ranged in size from 7-60 μm , with approximately 75% of all films observed
384 measuring less than 25 μm . Fragments were more varied in size, ranging from approximately 3-
385 165 μm . Over half (57%) of all fragments fell within the size range of 10-50 μm (Fig. 5).

386



387

388 **Fig. 5.** Size distributions of (a) fragments and (b) films, as well as example images of various
 389 MP morphologies observed: (c) beads, (d) fragments and (e) films. Size distributions represent
 390 all fragments and films observed across copepod samples from each sampling site.

391

392 The particle size distributions observed in the copepods were significantly different by sampling
 393 site and date (ANOSIM, $p = 0.001$). As can be seen in Fig. 3c, the size distribution of MP per
 394 100 copepods varied with date and sampling site. The smallest size class ($<10 \mu\text{m}$) predominates
 395 at Sites 5 on April 11 and at Sites 1 and 3 on April 16 and are observed in high concentrations at
 396 Site 6 on April 11. The next largest size class, $10\text{-}25 \mu\text{m}$, can be noted at Site 4 on April 11,
 397 while the $25\text{-}50 \mu\text{m}$ size MP were found in the highest amount at Sites 4 and 6 on April 11. The

398 50-100 μm size class was predominant at Site 1 on April 16. Across all sites, MP of the largest
399 size class ($> 100 \mu\text{m}$) were the least frequently observed.

400

401 *3.4. Comparison of microplastics in copepods and water*

402

403 The MP abundances observed in copepods were compared to MP concentrations we previously
404 reported in the water column (250-500 μm and 500-2000 μm) for paired samples (Bailey et al.,
405 2021), understanding these particles were larger than those bioavailable to the copepods. Smaller
406 MP were not analyzed in water column samples in our previous study because the nets used for
407 sampling had apertures of 80-153 μm to prevent clogging. No correlation was observed
408 between paired MP concentration for either size class studied in water and MP abundance in
409 zooplankton (both $p > 0.40$, Spearman Rank, Fig. A.1). nMDS demonstrated clustering by matrix
410 between polymer profiles observed in MP ingested by zooplankton and in small size class (250-
411 500 μm) of MP in water samples but not by sampling site (Fig. A.2, ANOSIM by matrix across
412 sites $p = 0.034$, by site $p = 0.23$).

413

414 *3.5. MP budgets in the system*

415

416 Here we make an estimate of the volume of MP in the guts of zooplankton in Raritan Bay and
417 use this to discuss a MP budget by contrasting estimates of the loading of MP to the Hudson-
418 Raritan system to the flux of MP through the zooplankton community. We note that this is a crude
419 order of magnitude estimate due to large uncertainties for select parameters. A first uncertainty is
420 estimating the volume of MP based on the reported size of MP in this paper, because the size

421 reflects the largest dimension, L , of each MP. Cozar et al. (2014) report a shape factor, $\alpha=0.1$, to
422 relate the volume of a single MP, $V_{mp}=\alpha L^3$. The reported size range, proportional to L^3 , for
423 particles larger than 5 mm was consistent with a constant shape factor across particle size
424 indicating that MP shapes are self-similar. With particles less than 1-2 mm the volume begins to
425 deviate from L^3 , but this was assumed to be due to loss of the smaller MP rather than a change in
426 the shape factor. The mean volume of plastics per zooplankton, was estimated using (Eq. 1;
427 Section 2.6) which yielded an estimate $V_p=8.6 \times 10^{-15} \text{ m}^3$.

428
429 A second uncertainty is the well-recognized spatial heterogeneity, or patchiness, of zooplankton
430 in marine systems (Folt and Burns, 1999). Such heterogeneity is apparent in Table 1 showing
431 total zooplankton and copepod abundances spanning two orders of magnitude and ranging from
432 58-5571 ind. m^{-3} . Over 90% of the zooplankton collected were copepods, with a mean
433 concentration from the sampling dates from our study of 1258 ind. m^{-3} , with more than half of
434 these (725 ind. m^{-3}) consisting of one of the three “select copepods (Table 1). The Bay’s surface
435 area is approximately $200 \times 10^6 \text{ m}^2$ with a mean depth of 5m and thus corresponds to an estimated
436 volume of 10^9 m^3 . Using the mean copepod abundance, we calculate that this corresponds to
437 1.2×10^{12} copepods and 7.25×10^{11} of the select copepods in the Bay, respectively. Thus, if our
438 estimates of MP present in the gut are representative of all the copepods in the Bay the total
439 volume of ingested plastics in copepods would be 0.011 m^3 , while for the select alone copepods
440 it would be 0.006 m^3 .

441
442 We estimated the volume of MP released annually into the Hudson-Raritan system to be 86.56
443 MT yr^{-1} . This estimate is based on estimate of US loadings to the marine systems (Meijer et al.,

444 2021) and human population residing in the Raritan (8.88M), Passaic (2.5M) and Hudson (8M)
445 rivers watersheds. Assuming that MP have a density close to 1000 kg m^{-3} we convert this loading
446 to $86.56 \text{ m}^3 \text{ yr}^{-1}$. We note that for the Raritan and Passaic Rivers alone, this method yields an
447 estimate of 8.88 and $18.5 \text{ m}^3 \text{ yr}^{-1}$, respectively, which is close to an estimate reported in Ravit et
448 al. (2017) of 12.6 and $26 \text{ m}^3 \text{ yr}^{-1}$ from these systems. If we apply a gut retention time of natural
449 food in zooplankton of 1 hour (ranges ~20-120 minutes for *Acartia* spp.; Kiørboe and Tiselius,
450 1987; Tirelli and Mayzaud, 2005), the above estimate of volume of MP ingested in zooplankton
451 corresponds to a flux of over $95 \text{ m}^3 \text{ yr}^{-1}$ of MP through the guts of copepod and $54 \text{ m}^3 \text{ yr}^{-1}$
452 through the guts of the select copepods alone.

453

454 **4. Discussion**

455

456 The results from the present study, which is the first to examine MP ingestion by dominant
457 zooplankton species in the highly urbanized Hudson-Raritan estuary, highlight the ubiquitous
458 nature of MP ingested by the lower levels of the food chain. MP were observed in every sample
459 analyzed. Although the presence of MP was consistently observed in every copepod sample
460 processed, the total number, size, morphology and polymer type of MP ingested by copepods,
461 and the relationship between ingestion incidence and copepod abundances, were highly variable
462 between sampling dates and site locations as well as between and among species. This is likely a
463 function of: 1) the generalist feeding nature of these species of copepods; and 2) highly variable
464 MP distributions, concentrations, polymer types, and sizes *in situ* (Bailey et al., 2021).

465

466 *4.1 MP ingested by copepods*

467
468 Ingestion incidence reported for copepods in the present study were higher than those reported
469 previously in other highly urbanized environments including copepods in the Yellow Sea (0.13
470 MP individual⁻¹; Sun et al., 2018a), copepods in the Terengganu Estuary and offshore waters of
471 Malaysia (<0.05 MP individual⁻¹; Taha et al., 2021), other zooplankton taxa from the Yellow Sea
472 and East China Sea (0.13-0.35 MP individual⁻¹ for amphipods, chaetognaths, and euphausiids;
473 Sun et al., 2018a, b), and amphipods, chaetognaths, fish larvae, and medusae in the Bohai Sea
474 (0.01-0.12 MP individual⁻¹; Zheng et al., 2020). Ingestion incidence reported for copepods in the
475 present study were also higher, for the exception of July 2018, than that found for copepods off
476 the coast of Kenya (0.33 MP individual⁻¹; Kosore et al., 2018). Higher ingestion incidences have
477 been observed, however, in marine stomapods (1.17 MP individual⁻¹; Sun et al., 2018b), marine
478 ichthyoplankton (1-27 MP individual⁻¹; Rodrigues et al., 2019; Steer et al., 2017), and
479 semiterrestrial amphipods in inland volcanic lakes (1.8-5 MP individual⁻¹; Iannilli et al., 2020).

480
481 The composition and morphology of MP ingested by zooplankton between the present study and
482 those conducted previously were highly variable. Polyethylene and polypropylene, the most
483 commonly ingested polymer types, were also the most dominant polymer types in surface water
484 samples (250-500 μm size class) analyzed in Bailey et al. (2021). The predominant polymer
485 types observed have densities less than (i.e., PE, PP, PDMS all $\rho < 0.97 \text{ g cm}^{-3}$) or near (i.e., PS
486 with $\rho = 0.96\text{-}1.05 \text{ g cm}^{-3}$) to 1 g cm^{-3} ; therefore, no relationship was observed between the
487 polymer buoyancy and ingestion by sampling site/salinity. And fragments (or beads in one study
488 site) were the most common MP morphology ingested in the present study, while fibers were not
489 observed. However, fibers (Sun et al., 2018a; Taha et al., 2021; Zheng et al., 2020) or filaments

490 (Kosore et al., 2018) dominated MP ingested by zooplankton in other studies. Furthermore, MP
491 consisting of cellophane dominated MP ingested by zooplankton in Zheng et al. (2020), while in
492 Sun et al. (2018a), organic oxidation polymers and poly-octenes accounted for nearly 50% of the
493 MP in zooplankton. This suggests the type of MP ingested is likely a function of the composition
494 of MP in surrounding seawater.

495
496 Size ranges of MP ingested by each copepod species was highly variable, particularly for the
497 larger copepods *A. tonsa* (adults = 800-1000 μm) and *C. typicus* (adults - 1000-2000 μm). These
498 two species are omnivorous and have been observed to feed on a large range of prey type and
499 size (*A. tonsa*: 2-250 μm , Berggreen et al., 1988; *C. typicus*: 3-300 μm , sometimes sizes up to
500 3600 μm , Calbet et al., 2007). MP ingested by the smallest species analyzed in the present study,
501 *P. crassirostris* (adults = 350-450 μm), mostly consisted of size ranges <50 μm . This species is
502 mainly herbivorous, grazing on nanophytoplankton 2-20 μm (Calbet et al., 2000), but has been
503 observed to feed on protozoans greater than 200 μm (Sant'Anna, 2013). In lab-based feeding
504 studies, when introduced to a range of sizes of MP polystyrene beads (2-17.9 μm), *P.*
505 *crassirostris* fed most efficiently on beads 7.0-7.9 μm (Ma et al., 2021). Therefore, the copepods
506 were likely not preferably selecting any one size class as prey but were instead feeding on the
507 sizes of particles (prey and MP), and MP type mentioned in the above paragraph, that were
508 present in the water column at the time. In the future, paired water and zooplankton sampling for
509 MP, specifically focused on the same MP size classes, should be conducted to better inform
510 whether copepods are more preferential or opportunistic in MP ingestion.

511

512 The particle sizes observed in copepod samples underscore the importance of using Raman
513 microscopy for MP analysis for this matrix rather than FTIR. MP smaller than 25 μm comprised
514 between 23-77% of all MP observed across all species and sampling sites studied (Fig. 3c). This
515 size class is near the diffraction limit of FTIR microscopy. Particles smaller than 10 μm are
516 below the diffraction limit of FTIR and can only be effectively studied using Raman microscopy.

517

518 It should be noted that concentrated nitric acid, the digestion agent used to isolate MP ingested
519 by copepods in the present study, has been documented to depolymerize or solubilize particular
520 polymer types (e.g., polyurethanes, polyethers and diene polymers/rubbers) and cause particle
521 fragmentation of polymers such as polyesters (e.g., PET) and polyamides (e.g., Nylon 66)
522 (Enders et al., 2017; Thiele et al., 2019). We initially attempted an enzymatic digestion using
523 proteinase-K according to Cole et al. (2014); However, the digested samples contained large
524 amounts of residual exoskeleton (chitin) that made visual identifications of MP difficult
525 compared to those digested using nitric acid (Sipps and Arbuckle-Keil, 2021). Thus, the values
526 presented here may be underestimates of total MP ingested due to the breakdown of certain
527 polymers during the acid digestion. Sizes of polyester and polyamide MP may also be skewed
528 toward smaller size classes and higher particle counts may have been observed due to
529 fragmentation of large particles into multiple smaller particles during digestion.

530

531 *4.2 MP budgets in the system*

532

533 Based on the calculated fluxes of MP through the guts of copepods, one could conclude then that
534 the copepod community alone could process the annual loadings of MP to this system, although

535 we note that there will be considerable temporal variability to this based on zooplankton
536 phenology. Notably, in addition to those described above, an additional uncertainty in this
537 calculation is the gut retention time of MP in zooplankton. Cole et al. (2013) found variable gut
538 retention time of MP for copepods with some gut retention time similar to natural foods (hours)
539 while others retained within guts for weeks and that irregularly-shaped microplastics may
540 become entangled within the intestinal track and increase gut retention time. Indeed, numerous
541 studies (referenced in Cole et al., 2013) found long or even ‘near-indefinite’ gut retention times
542 in marine wildlife and that prolonged gut-retention times. Thus, as gut retention time increases
543 the fraction of MP loadings that passes through the guts of zooplankton decreases. In the case of
544 a short gut retention time, we suggest that large fraction of MP discharged into this system would
545 be pass through the guts of zooplankton and be incorporated into sinking fecal pellets and
546 retained in the system due to the strong tendency for estuarine systems to trap settling particles
547 (Burchard et al., 2018). In contrast, if gut residence time is long, most of the positively buoyant
548 MP would be discharged into the coastal ocean. Based on Cole et al. (2013) indicating variable
549 gut residence of MP, we suggest that reality lies between these two extremes. Yet, while more
550 research is needed to better quantify the impact of zooplankton on the fate and transport of MP,
551 the mere possibility that zooplankton feeding could constrain the transport of MP between land
552 and sea is remarkable.

553

554 **5. Broader Significance**

555

556 Zooplankton are not only key players in the ocean food web, transferring energy from primary
557 producers to higher trophic levels, but they also play a critical role in the recycling and export of

558 nutrients (Steinberg and Saba, 2008; Mitra et al., 2014; Turner, 2015). As such, MP ingestion by
559 zooplankton can have important implications on MP fate and transport. Ordinarily buoyant MP
560 particles may be repackaged in fecal pellets excreted by the zooplankton, altering the
561 bioavailability of the MP to organisms throughout the water column (Cole et al., 2016).
562 Furthermore, the incorporation of MP in fecal pellets can alter the pellets' densities and sinking
563 rates, disrupting the vertical transport of organic matter and nutrients in the water column that is
564 an integral part of the biological pump (Cole et al., 2016; Coppock et al., 2019; Shore et al.,
565 2021) The "sink" of MP through the food web is one possible mechanism for the large mis-
566 match between the total loadings of plastics to the marine environment and the vastly smaller
567 global inventory of plastics at the ocean's surface (Cózar et al., 2014).

568
569 Expanded studies investigating the potential for other zooplankton species to ingest MP, along
570 with MP ingestion occurrence and transit times of MP in zooplankton guts would be highly
571 valuable in determining, on a community level, the comprehensive role of zooplankton in MP
572 bioaccumulation through the food web and transport and fate in aquatic systems.

573

574 **Acknowledgements**

575

576 We thank Captain Chip Haldeman of the R/V *Rutgers* for his field support. We also thank
577 Rutgers University undergraduates Paul Coyne and Madelyn Engelman for their assistance in
578 zooplankton sample processing.

579

580 **Funding sources**

581

582 This manuscript is the result of research sponsored by the New Jersey Sea Grant Consortium
583 (NJSGC) with funds from the National Oceanic and Atmospheric Administration (NOAA)
584 Office of Sea Grant, U.S. Department of Commerce [NA18OAR170087]. The statements,
585 findings, conclusions, and recommendations are those of the author(s) and do not necessarily
586 reflect the views of the NJSGC or the U.S. Department of Commerce. Additional funding was
587 provided by the Hudson River Foundation Tibor T. Polgar Award to KS.

588

589 Dataset

590

591 MP data collected during the present study are available in the Rutgers University CORE data
592 repository ([dataset] Arbuckle-Keil, 2021).

593

594 **References**

- 595
- 596 Alfaro-Núñez, A., Astorga, D., Cáceres-Farías, L., Bastidas, L., Villegas, C.S., Macay, K.,
 597 Christensen, J.H., 2021. Microplastic pollution in seawater and marine organisms across
 598 the Tropical Eastern Pacific and Galápagos. *Sci. Rep.* 11: 6424.
 599 <https://doi.org/10.1038/s41598-021-85939-3>.
- 600 Alimi, O.S, Budarz, J.F., Hernandez, L.M., Tufenkji, N., 2018. Microplastics and nanoplastics in
 601 aquatic environments: aggregation, deposition, and enhanced contaminant transport.
 602 *Environ. Sci. Technol.* 52: 1704-1724. <https://doi.org/10.1021/acs.est.7b05559>.
- 603 Andrady, A.L., 2011. Microplastics in the marine environment. *Mar. Pollut. Bull.* 62: 1596-1605.
 604 <https://doi.org/10.1016/j.marpolbul.2011.05.030>.
- 605 Arbuckle-Keil, G., 2021. Supporting information for: Pervasive occurrence of microplastics in
 606 Raritan-Hudson estuary zooplankton. Rutgers University CORE data repository.
 607 doi:10.7282/00000135.
- 608 Avio, C.G., Gorbi, S., Regoli, F., 2016. Plastics and microplastics in the oceans: From emerging
 609 pollutants to emerged threat. *Mar. Environ. Res.* 128: 2-11.
 610 <https://doi.org/10.1016/j.marenvres.2016.05.012>.
- 611 Bailey, K., Sipps, K., Saba, G.K., Arbuckle-Keil, G., Chant, R.J., Fahrenfeld, N.L., 2021.
 612 Quantification and composition of microplastics in the Raritan Hudson Estuary:
 613 Comparison to pathways of entry and implications for fate. *Chemosphere* 272: 129886.
 614 <https://doi.org/10.1016/j.chemosphere.2021.129886>.
- 615 Berggreen, U., Hansen, B., Kiørboe, T., 1988. Food size spectra, ingestion and growth of the
 616 copepod *Acartia tonsa* during development: Implications for determination of copepod
 617 production. *Mar. Biol.* 99: 341-352. <https://doi.org/10.1007/BF02112126>.
- 618 Botterell, Z.L.R., Beaumont, N., Dorrington, T., Steinke, M., Thompson, R.C., Lindeque, P.K.,
 619 2019. Bioavailability and effects of microplastics on marine zooplankton: A review.
 620 *Environ. Pollut.* 245: 98-110. <https://doi.org/10.1016/j.envpol.2018.10.065>.
- 621 Boucher, J., Friot, D., 2017. Primary Microplastics in the Oceans: A Global Evaluation of
 622 Sources. Gland, Switzerland.
- 623 Burchard, H., Schuttelaars, H.M., Ralston, D.K., 2018. Sediment trapping in estuaries. *Ann. Rev.*
 624 *Mar. Sci.* 10: 371-395. <https://doi.org/10.1146/annurev-marine-010816-060535>.
- 625 Burns, E.E., Boxall, A.B.A., 2018. Microplastics in the aquatic environment: evidence for or
 626 against adverse impacts and major knowledge gaps. *Environ. Toxicol. Chem* 37(11):
 627 2776-2796. <https://doi.org/10.1002/etc.4268>.
- 628 Calbet, A., Carlotti, F., Gaudy, R., 2007. The feeding ecology of the copepod *Centropages*
 629 *typicus* (Kröyer). *Prog. Oceanogr.* 72: 137-150.
 630 <https://doi.org/10.1016/j.pocean.2007.01.003>.
- 631 Calbet, C.J., Landry, M.R., Scheinberg, R.D., 2000. Copepod grazing in a subtropical bay:
 632 species-specific responses to a midsummer increase in nanoplankton standing stock. *Mar.*
 633 *Ecol. Prog. Ser.* 193: 75-84. doi: 10.3354/meps193075.
- 634 Clark, J.R., Cole, M., Lindeque, P.K., Fileman, E., Blackford, J., Lewis, C., Lenton, T.M.,
 635 Galloway, T.S., 2016. Marine microplastic debris: a targeted plan for understanding and
 636 quantifying interactions with marine life. *Front. Ecol. Environ.* 14 (6): 317-324.
 637 <https://doi.org/10.1002/fee.1297>.
- 638 Cole, M., Coppock, R., Lindeque, P.K., Altin, D., Reed, S., Pond, D.W., Sørensen, L., Galloway,
 639 T.S., Booth, A.M., 2019. Effects of nylon microplastic on feeding, lipid accumulation,

- 640 and moulting in a coldwater copepod. *Environ. Sci. Technol.* 53: 7075-7082.
641 <https://doi.org/10.1021/acs.est.9b01853>.
- 642 Cole, M., Lindeque, P., Fileman, E., Clark, J., Lewis, C., Halsband, C., Galloway T.S., 2016.
643 Microplastics alter the properties and sinking rates of zooplankton faecal pellets. *Environ.*
644 *Sci. Technol.* 50: 3239-3246. <https://doi.org/10.1021/acs.est.5b05905>.
- 645 Cole, M., Lindeque, P., Fileman, E., Halsband, C., Galloway, T.S., 2015. The impact of
646 polystyrene microplastics on feeding, function and fecundity in the marine copepod
647 *Calanus helgolandicus*. *Environ. Sci. Technol.* 49: 1130-1137.
648 <https://doi.org/10.1021/es504525u>.
- 649 Cole, M., Lindeque, P., Fileman, E., Halsband, C., Goodhead, R., Moger, J., Galloway, T.S.,
650 2013. Microplastic ingestion by zooplankton. *Environ. Sci. Technol.* 47(12): 6646-6655.
651 <https://doi.org/10.1021/es400663f>.
- 652 Cole, M., Lindeque, P., Halsband, C., Galloway, T.S., 2011. Microplastics as contaminants in the
653 marine environment: A review. *Mar. Pollut. Bull.* 62: 2588-2597.
654 <https://doi.org/10.1016/j.marpolbul.2011.09.025>.
- 655 Cole, M., Webb, H., Lindeque, P.K., Fileman, E.S., Halsband, C., Galloway, T.S., 2014.
656 Isolation of microplastics in biota-rich sweater samples and marine organisms. *Sci.*
657 *Reports* 4: 4528. doi: 10.1038/srep04528.
- 658 Coppock, R.L., Galloway, T.S., Cole, M., Fileman, E.S., Queirós, A.M., Lindeque, P.K., 2019.
659 Microplastics alter feeding selectivity and faecal density in the copepod, *Calanus*
660 *helgolandicus*. *Sci. Total Environ.* 687: 780-789.
661 <https://doi.org/10.1016/j.scitotenv.2019.06.009>.
- 662 Costa, E., Piazza, V., Lavorano, S., Faimali, M., Garaventa, F., Gambardella, C., 2020. Trophic
663 transfer of microplastics from copepods to jellyfish in the marine environment. *Front.*
664 *Environ. Sci.* 8: 571732. <https://doi.org/10.3389/fenvs.2020.571732>.
- 665 Cowger, W., Steinmetz, Z., Gray, A., Munno, K., Lynch, J., Hapich, H., Primpke, S., De Frond,
666 H., Rochman, C., Herodotou, O., 2021. Microplastic spectral classification needs an open
667 source community: Open Specy to the rescue! *Anal. Chem.* 93, 21, 7543-7548.
668 <https://doi.org/10.1021/acs.analchem.1c00123>.
- 669 Cózar, A., Echevarría, F., González-Gordillo, J.I., Irigoien, X., Ubeda, B., Hernández-León, S,
670 Palma, A.T., Navarro, S., García-de-Lomas, J., Ruiz, A., Fernández-de-Puelles, M.L.,
671 Duarte, C.M., 2014. Plastic debris in the open ocean. *Proc. Natl. Acad. Sci. USA* 111:
672 10239-10244. <https://doi.org/10.1073/pnas.1314705111>.
- 673 Crespy, D., Bozonnet, M., Meier, M., 2008. 100 Years of Bakelite, the Material of a 1000 Uses.
674 *Angewandte Chemie International Edition* 47: 3322-3328.
675 <https://doi.org/10.1002/anie.200704281>.
- 676 Derraik, J.G.B., 2002. The pollution of the marine environment by plastic debris: a review. *Mar.*
677 *Pollut. Bull.* 44: 842-852. [https://doi.org/10.1016/S0025-326X\(02\)00220-5](https://doi.org/10.1016/S0025-326X(02)00220-5).
- 678 Desforges, J.-P.W., Galbraith, M., Ross, P.S., 2015. Ingestion of microplastics by zooplankton in
679 the Northeast Pacific Ocean. *Arch. Environ. Contam. Toxicol.* 69: 320-330.
680 <https://doi.org/10.1007/s00244-015-0172-5>.
- 681 Dusaucy, J., Gateuille, D., Perrette, Y., Naffrechoux, E., 2021. Microplastic pollution of
682 worldwide lakes. *Environ. Pollut.* 284: 117075.
683 <https://doi.org/10.1016/j.envpol.2021.117075>.

- 684 Enders, K., Lenz, R., Beer, S., Stedmon, C.A., 2016. Extraction of microplastic from biota:
685 recommended acidic digestion destroys common plastic polymers. *ICES J. Mar. Sci.* 74
686 (1): 326-331. <https://doi.org/10.1093/icesjms/fsw173>.
- 687 Farrell, P., Nelson, K., 2013. Trophic level transfer of microplastic: *Mytilus edulis* (L.) to
688 *Carcinus maenas* (L.). *Environ. Pollut.* 177: 1-3.
689 <https://doi.org/10.1016/j.envpol.2013.01.046>.
- 690 Frias, J.P.G.L., Otero, V., Sobral, P., 2014. Evidence of microplastics in samples of zooplankton
691 from Portuguese coastal waters. *Mar. Environ. Res.* 95: 89-95.
692 <https://doi.org/10.1016/j.marenvres.2014.01.001>.
- 693 Foley, C.J., Feiner, Z.S., Malinich, T.D., Höök, T.O., 2018. A meta-analysis of the effects of
694 exposure to microplastics on fish and aquatic invertebrates. *Sci. Total Environ.*
695 631-632: 550-559. <https://doi.org/10.1016/j.scitotenv.2018.03.046>.
- 696 Iannilli, V., Corami, F., Grasso, P., Lecce, F., Buttinelli, M., Setini, A., 2020. Plastic abundance
697 and seasonal variation on the shorelines of three volcanic lakes in Central Italy: can
698 amphipods help detect contamination? *Environ. Sci. Pollut. Res.* 27: 14711-14722.
699 <https://doi.org/10.1007/s11356-020-07954-7>.
- 700 Jeffries, H.P., 1964. Comparative Studies on Estuarine Zooplankton. *Limnol. Oceanogr.* 9: 348-
701 358. <https://doi.org/10.4319/lo.1964.9.3.0348>.
- 702 Jeong, C.B., Kang, H.M., Lee, M.C., Kim, D.H., Han, J., Hwang, D.S., Souissi, S., Lee, S.J.,
703 Shin, K.H., Park, H.G., Lee, J.S., 2017. Adverse effects of microplastics and oxidative
704 stress-induced MAPK/Nrf2 pathway-mediated defense mechanisms in the marine
705 copepod *Paracyclops nana*. *Sci. Rep.* 7: 1-11. <https://doi.org/10.1038/srep41323>.
- 706 Kanhai, L.D.K., Johansson, C., Frias, J.P.G.L., Gardfeldt, K., Thompson, R.C., O'Connor, I.,
707 2019. Deep sea sediments of the Arctic Central Basin: A potential sink for microplastics.
708 *Deep-Sea Res. I* 145: 137-142. <https://doi.org/10.1016/j.dsr.2019.03.003>.
- 709 Kiørboe, T., Tiselius, P.T., 1987. Gut clearance and pigment destruction in a herbivorous
710 copepod, *Acartia tonsa*, and the determination of *in situ* grazing rates. *J. Plankton Res.* 9:
711 525-534. <https://doi.org/10.1093/plankt/9.3.525>.
- 712 Kosore, C., Ojwang, L., Maghanga, J., Kamau, J., Kimeli, A., Omukoto, J., Ngisiag'e, N.,
713 Mwaluma, J., Ong'ada, H., Magori, C., 2018. Occurrence and ingestion of microplastics
714 by zooplankton in Kenya's marine environment: first documented evidence. *Afr. J. Mar.*
715 *Sci.* 40: 225-234. <https://doi.org/10.2989/1814232X.2018.1492969>.
- 716 Kvale, K., Prowe, A.E.F., Chien, C.-T., Landolfi, A., Oschlies, A. 2020. The global biological
717 microplastic particle sink. *Sci. Reports* 10: 16670. <https://doi.org/10.1038/s41598-020-72898-4>.
- 718
- 719 Lee, K.W., Raisuddin, S., Hwang, D.S., Park, H.G., Dahms, H.U., Ahn, I.Y., Lee, J.S., 2008.
720 Two-generation toxicity study on the copepod model species *Tigriopus japonicus*.
721 *Chemosphere* 72: 1359-1365. <https://doi.org/10.1016/j.chemosphere.2008.04.023>.
- 722 Ma, X., Jacoby, C.A., Johnson, K.B., 2021. Grazing by the copepod *Parvocalanus crassirostris*
723 on *Picochlorum* sp. at harmful bloom densities and the role of particle size. *Front. Mar.*
724 *Sci.* 8: 664154. <https://doi.org/10.3389/fmars.2021.664154>.
- 725 Masura, J., Baker, J., Foster, G., Arthur, C., Herring, C., Editor, T., 2015. Laboratory methods
726 for the analysis of microplastics in the marine environment: recommendations for
727 quantifying synthetic particles in waters and sediments. NOAA Technical Memorandum
728 NOS-OR&R-48. [https://marinedebris.noaa.gov/sites/default/files/publications-](https://marinedebris.noaa.gov/sites/default/files/publications-files/noaa_microplastics_methods_manual.pdf)
729 [files/noaa_microplastics_methods_manual.pdf](https://marinedebris.noaa.gov/sites/default/files/publications-files/noaa_microplastics_methods_manual.pdf).

- 730 Meijer, L.J.J., van Emmerik, T., van der Ent, R., Schmidt, C., Lebreton, L., 2021. More than
731 1000 rivers account for 80% of global riverine plastic emissions into the ocean. *Sci. Adv.*
732 7: eaaz5803. doi: 10.1126/sciadv.aaz5803.
- 733 Mitra, A., Castellani, C., Gentleman, W.C., Jónasdóttir, S.H., Flynn, K.J., Bode, A., Halsband,
734 C., Kuhn, P., Licandro, P., Agersted, M.D., Calbet, A., Lindeque, P.K., Koppelman, R.,
735 Møller, E.F., Gislason, A., Nielsen, T.G., St. John, M., 2014. Bridging the gap between
736 marine biogeochemical and fisheries sciences; configuring the zooplankton link. *Prog.*
737 *Oceanogr.* 129 B: 176-199. <https://doi.org/10.1016/j.pocean.2014.04.025>.
- 738 Moore, C.J., Moore, S.L., Leecaster, M.K., Weisberg, S.B., 2001. A comparison of plastic and
739 plankton in the North Pacific Central Gyre. *Mar. Pollut. Bull.* 42(12): 1297-1300.
740 [https://doi.org/10.1016/S0025-326X\(01\)00114-X](https://doi.org/10.1016/S0025-326X(01)00114-X).
- 741 Nel, H.A., Dalu, T., Wasserman, R.J., 2018. Sinks and sources: Assessing microplastic
742 abundance in river sediment and deposit feeders in an Austral temperate urban river
743 system. *Sci. Total Environ.* 612: 950-956.
744 <https://doi.org/10.1016/j.scitotenv.2017.08.298>.
- 745 Pastorino, P., Pizzul, E., Bertoli, M., Anselmi, S., Kušće, M., Menconi, V., Prearo, M., Renzi,
746 M., 2021. First insights into plastic and microplastic occurrence in biotic and abiotic
747 compartments, and snow from a high-mountain lake (Carnic Alps). *Chemosphere* 265:
748 12921. <https://doi.org/10.1016/j.chemosphere.2020.129121>.
- 749 Ravit, B., Cooper, K., Moreno, G., Buckley, B., Yang, I., Deshpande, A., Meola, S., Jones, D.,
750 Hsieh, A., 2017. Microplastics in urban New Jersey freshwaters: distribution, chemical
751 identification, and biological affects. *AIMS Environ. Sci.* 4(6): 809-826. doi:
752 10.3934/environsci.2017.6.809.
- 753 Rodrigues, S., Almeida, C.M.R., Silva, D., Cunha, J., Antunes, C., Freitas, V., Ramos, S., 2019.
754 Microplastic contamination in an urban estuary: abundance and distribution of
755 microplastics and fish larvae in the Douro estuary. *Sci. Total Environ.* 659: 1071-1081.
756 <https://doi.org/10.1016/j.scitotenv.2018.12.273>.
- 757 Rodrigues, S.M., Elliott, M., Almeida, C.M.R., Ramos, S., 2021. Microplastics and plankton:
758 Knowledge from laboratory and field studies to distinguish contamination from pollution.
759 *J. Hazard. Mater.* 417: 126057. <https://doi.org/10.1016/j.jhazmat.2021.126057>.
- 760 Rothenberger, M.B., Swaffield, T., Calomeni, A.J., Cabrey, C.D., 2014. Multivariate Analysis of
761 Water Quality and Plankton Assemblages in an Urban Estuary. *Estuaries Coast.* 37: 695-
762 711. <https://doi.org/10.1007/s12237-013-9714-0>.
- 763 Sant' Anna, E.E., 2013. Remains of the protozoan *Sticholonche zanclea* in the faecal
764 pellets of *Paracalanus quasimodo*, *Parvocalanus crassirostris*, *Temora stylifera* and
765 *Temora turbinata* (Copepoda, Calanoida) in Brazilian coastal waters. *Braz. J. Oceanogr.*
766 61: 73-76. doi: 10.1590/S1679-87592013000100008.
- 767 Savoca, M.S., McInturf, A.G., Hazen, E.L., 2021. Plastic ingestion by marine fish is widespread
768 and increasing. *Glob. Change Biol.* 27: 2188-2199. <https://doi.org/10.1111/gcb.15533>.
- 769 Setälä, O., Fleming-Lehtinen, V., Lehtiniemi, M., 2014. Ingestion and transfer of microplastics
770 in the planktonic food web. *Environ. Pollut.* 185: 77-83.
771 <https://doi.org/10.1016/j.envpol.2013.10.013>.
- 772 Shore, E.A., deMayo, J.A., Pespeni, M.H., 2021. Microplastics reduce net population growth and
773 fecal pellet sinking rates for the marine copepod *Acartia tonsa*. *Environ. Poll.* 284:
774 117379. <https://doi.org/10.1016/j.envpol.2021.117379>.

- 775 Sipps, K., Arbuckle-Keil, G., 2021. Spectroscopic Characterization and Quantification of
776 Microplastics in the Hudson River. Section VII: 1-37 pp. In: Yozzo, D.J., Fernald, S.H.,
777 Andreyko, H., Eds., Final Reports of the Tibor T. Polgar Fellowship Program, 2019.
778 Hudson River Foundation. [https://www.hudsonriver.org/wp-](https://www.hudsonriver.org/wp-content/uploads/2021/08/Polgar-Final-Reports-2019.pdf)
779 [content/uploads/2021/08/Polgar-Final-Reports-2019.pdf](https://www.hudsonriver.org/wp-content/uploads/2021/08/Polgar-Final-Reports-2019.pdf)
- 780 Socrates, G., 2004. Infrared and Raman Characteristic Group Frequencies: Tables and Charts, 3rd
781 Edition. Wiley, Chichester, United Kingdom.
- 782 Steer, M., Cole, M., Thompson, R.C., Lindeque, P.K., 2017. Microplastic ingestion in fish larvae
783 in the western English Channel. *Environ. Pollut.* 226: 250-259.
784 <https://doi.org/10.1016/j.envpol.2017.03.062>.
- 785 Steinberg, D.K., Saba, G.K., 2008. Nitrogen consumption and metabolism in marine
786 zooplankton. In: Capone, D.G., Bronk, D.A., Mulholland, M.R., Carpenter, E.J., Eds.,
787 Nitrogen in the Marine Environment, 2nd Edition. Academic Press, Boston.
- 788 Stepien, J.C., Malone, T.C., Chervin, M.B., 1981. Copepod communities in the estuary and
789 coastal plume of the Hudson River. *Estuar. Coast. Shelf Sci.* 13: 185-195.
790 [https://doi.org/10.1016/S0302-3524\(81\)80075-8](https://doi.org/10.1016/S0302-3524(81)80075-8).
- 791 Sun, X., Liang, J., Zhu, M., Zhao, Y., Zhang, B., 2018a. Microplastics in seawater and
792 zooplankton from the Yellow Sea. *Environ. Pollut.* 242: 585-595.
793 <https://doi.org/10.1016/j.envpol.2018.07.014>.
- 794 Sun, X., Liu, T., Zhu, M., Liang, J., Zhao, Y., Zhang, B., 2018b. Retention and characteristics of
795 microplastics in natural zooplankton taxa from the East China Sea. *Sci. Total Environ.*
796 640: 232-242. <https://doi.org/10.1016/j.scitotenv.2018.05.308>.
- 797 Svetlichny, L., Isinibilir, M., Mykitchak, T., Eryalçın, K.M., Türkeri, E.E., Yuksel, E., Kideys,
798 A.E., 2021. Microplastic consumption and physiological response in *Acartia clausi* and
799 *Centropages typicus*: possible roles of feeding mechanisms. *Reg. Stud. Mar. Sci.* 43:
800 101650. <https://doi.org/10.1016/j.rsma.2021.101650>.
- 801 Taha, Z.D., Amin, R.M., Anuar, S.T., Nasser, A.A.A., Sohaimi, E.S., 2021. Microplastics in
802 seawater and zooplankton: A case study from Terengganu estuary and offshore waters,
803 Malaysia. *Sci. Total Environ.* 786: 147466.
804 <https://doi.org/10.1016/j.scitotenv.2021.147466>.
- 805 Thiele, C.J., Hudson, M.D., Russell, A.E., 2019. Evaluation of existing methods to extract
806 microplastics from bivalve tissue: Adapted KOH digestion protocol improves filtration at
807 single-digit pore size. *Mar. Pollut. Bull.* 142: 384-393.
808 <https://doi.org/10.1016/j.marpolbul.2019.03.003>.
- 809 Tirelli, V., Mayzaud, P., 2005. Relationship between functional response and gut transit time in
810 the calanoid copepod *Acartia clausi*: role of food quantity and quality. *J. Plankton Res.*
811 27: 557-568. <https://doi.org/10.1093/plankt/fbi031>.
- 812 Turner, J. T. 2015. Zooplankton fecal pellets, marine snow, phytodetritus and the ocean's
813 biological pump. *Aquat. Microb. Ecol.* 27: 57-102.
814 <https://doi.org/10.1016/j.pocean.2014.08.005>.
- 815 United States Environmental Protection Agency. 2021. Facts and figures about materials, waste
816 and recycling. Plastics: Material-specific data. [https://www.epa.gov/facts-and-figures-](https://www.epa.gov/facts-and-figures-about-materials-waste-and-recycling/plastics-material-specific-data)
817 [about-materials-waste-and-recycling/plastics-material-specific-data](https://www.epa.gov/facts-and-figures-about-materials-waste-and-recycling/plastics-material-specific-data) (accessed 18 August
818 2021).

- 819 Van Colen, C., Vanhove, B., Diem, A., Moens, T., 2020. Does microplastic ingestion by
820 zooplankton affect predator-prey interactions? An experimental study on larviphagy.
821 *Environ. Pollut.* 256: 113479. <https://doi.org/10.1016/j.envpol.2019.113479>.
- 822 Vroom, R.J.E., Koelmans, A.A., Besseling, E., Halsband, C., 2017. Aging of microplastics
823 promotes their ingestion by marine zooplankton. *Environ. Pollut.* 231: 987-996.
824 <https://doi.org/10.1016/j.envpol.2017.08.088>.
- 825 Waller, C.L., Griffiths, H.J., Waluda, C.M., Thorpe, S.E., Loaiza, I., Moreno, B., Pacherres,
826 C.O., Hughes, K.A., 2017. Microplastics in the Antarctic marine system: An emerging
827 area of research. *Sci. Total Environ.* 598: 220-227.
828 <https://doi.org/10.1016/j.scitotenv.2017.03.283>.
- 829 Wesch, C., Elert, A.M., Wörner, M., Braun, U., Klein, R., Paulus, M., 2017. Assuring quality in
830 microplastic monitoring: About the value of clean-air devices as essentials for verified
831 data. *Sci. Rep.* 7: 5424. <https://doi.org/10.1038/s41598-017-05838-4>.
- 832 Woodall, L.C., Gwinnett, C., Packer, M., Thompson, R.C., Robinson, L.F., Paterson, G.L.J.,
833 2015. Using a forensic science approach to minimize environmental contamination and to
834 identify microfibrils in marine sediments. *Mar. Pollut. Bull.* 95: 40-46.
835 <https://doi.org/10.1016/j.marpolbul.2015.04.044>.
- 836 Woodall, L.C., Sanchez-Vidal, A., Canals, M., Paterson, G.L.J., Coppock, R., Sleight, V.,
837 Calafat, A., Rogers, A.D., Narayanaswamy, B.E., Thompson, R.C., 2014. The deep sea is
838 a major sink for microplastic debris. *R. Soc. open sci* 1: 140317.
839 <http://dx.doi.org/10.1098/rsos.140317>.
- 840 Wright, S.L., Thompson, R.C., Galloway, T.S., 2013. The physical impacts of microplastics on
841 marine organisms: A review. *Environ. Poll.* 178: 483-492.
842 <https://doi.org/10.1016/j.envpol.2013.02.031>.
- 843 Yu, J., Tian, J.Y., Xu, R., Zhang, Z.Y., Yang, G.P., Wang, X.D., Lai, J.G., Chen, R., 2020.
844 Effects of microplastics exposure on ingestion, fecundity, development, and
845 dimethylsulfide production in *Tigriopus japonicus* (Harpacticoida, copepod). *Environ.*
846 *Pollut.* 267: 115429. <https://doi.org/10.1016/j.envpol.2020.115429>.
- 847 Zhang, C., Jeong, C.B., Lee, J.S., Wang, D., Wang, M., 2019. Transgenerational proteome
848 plasticity in resilience of a marine copepod in response to environmentally relevant
849 concentrations of microplastics. *Environ. Sci. Technol.* 53: 8426-8436.
850 <https://doi.org/10.1021/acs.est.9b02525>.
- 851 Zhao, S., Zhu, L., Wang, T., Li, D., 2014. Suspended microplastics in the surface water of the
852 Yangtze Estuary system, China: first observations on occurrence, distribution. *Mar.*
853 *Pollut. Bull.* 86(1): 562-568. <https://doi.org/10.1016/j.marpolbul.2014.06.032>.
- 854 Zheng, S., Zhao, Y., Liangwei, W., Liang, J., Liu, T., Zhu, M., Li, Q., Sun, X., 2020.
855 Characteristics of microplastics ingested by zooplankton from the Bohai Sea, China. *Sci.*
856 *Total Environ.* 713: 136357. <https://doi.org/10.1016/j.scitotenv.2019.136357>.
- 857
858
859
860
861
862
863

